# Neutrophil infiltration leads to fetal growth restriction by impairing the placental vasculature in DENV-infected pregnant mice

Yingying Zhang,[a,b,i] Ziyang Sheng,[a,**,i] Qiaozhu Chen,[c,i] Anni Zhou,[d,i] Jiaying Cao,[a] Feiyang Xue,[a] Yanzhen Ye,[e] Na Wu,[f] Na Gao,[a] Dongying Fan,[a] Libo Liu,[a] Yuetong Li,[a] Peigang Wang,[a] Li Liang,[g] Deshan Zhou,[h] Fuchun Zhang,[g] Fang Li,[c,g,***] and Jing An[a,*]

[a]Department of Microbiology, School of Basic Medical Sciences, Capital Medical University, Beijing, 100069, China
[b]Department of Blood Transfusion, Sir Run Run Shaw Hospital, Zhejiang University School of Medicine, Hangzhou, China
[c]Department of Ob&Gyn, Guangzhou Women and Children's Medical Center, Guangzhou Medical University, Guangzhou, China
[d]Beijing Key Laboratory for Precancerous Lesion of Digestive Disease, Department of Gastroenterology, National Clinical Research Center for Digestive Disease, Beijing Digestive Disease Center, Beijing Friendship Hospital, Capital Medical University, Beijing, China
[e]Department of Obstetrics and Gynecology, People's Hospital of Nanhai District, Foshan City, 528200, Guangdong, China
[f]Laboratory Animal Center, Capital Medical University, Beijing, 100069, China
[g]Guangzhou Eighth People's Hospital, Guangzhou Medical University, Guangzhou, China
[h]Department of Histology and Embryology, School of Basic Medical Sciences, Capital Medical University, Beijing, China

eBioMedicine
2023;95: 104739
Published Online xxx
https://doi.org/10.1016/j.ebiom.2023.104739

## Summary

**Background** Dengue virus (DENV) infection during pregnancy increases the risk of adverse fetal outcomes, which has become a new clinical challenge. However, the underlying mechanism remains unknown.

**Methods** The effect of DENV-2 infection on fetuses was investigated using pregnant interferon α/β receptor-deficient (*Ifnar1*$^{-/-}$) mice. The histopathological changes in the placentas were analyzed by morphological techniques. A mouse inflammation array was used to detect the cytokine and chemokine profiles in the serum and placenta. The infiltration characteristics of inflammatory cells in the placentas were evaluated by single-cell RNA sequencing.

**Findings** Fetal growth restriction observed in DENV-2 infection was mainly caused by the destruction of the placental vasculature rather than direct damage from the virus in our mouse model. After infection, neutrophil infiltration into the placenta disrupts the expression profile of matrix metalloproteinases, which leads to placental dysvascularization and insufficiency. Notably, similar histopathological changes were observed in the placentas from DENV-infected puerperae.

**Interpretation** Neutrophils play key roles in placental histopathological damage during DENV infection, which indicates that interfering with aberrant neutrophil infiltration into the placenta may be an important therapeutic target for adverse pregnancy outcomes in DENV infection.

**Funding** The National Key Research and Development Plans of China (2021YFC2300200-02 to J.A., 2019YFC0121905 to Q.Z.C.), the National Natural Science Foundation of China (NSFC) (U1902210 and 81972979 to J. A., 81902048 to Z. Y. S., and 82172266 to P.G.W.), and the Support Project of High-level Teachers in Beijing Municipal Universities in the Period of 13th Five-year Plan, China (IDHT20190510 to J. A.).



**Keywords:** Dengue virus; Adverse pregnancy outcomes; Placenta; Neutrophil; Matrix metalloproteinase

*Corresponding author.
**Corresponding author.
***Corresponding author. Department of Ob&Gyn, Guangzhou Women and Children's Medical Center, Guangzhou Medical University, Guangzhou, China.
*E-mail addresses:* anjing@ccmu.edu.cn (J. An), shengzy@ccmu.edu.cn (Z. Sheng), gz8hlf@126.com (F. Li).
[i]These authors contributed equally to this work.

## Research in context

### Evidence before this study

Dengue is endemic in more than 100 countries and is spreading to new areas. Recently, there are more and more reports about pregnant women infected with dengue virus (DENV), which is linked to adverse fetal outcomes. However, most studies on adverse pregnancy outcomes associated with maternal DENV infection have focused on clinical phenotypic features, and the mechanisms of fetal complications remain unclear.

### Added value of this study

1. The predominant manifestations of fetal intrauterine growth restriction caused by DENV-2 infection in pregnant mice are low body weight, anemia, and multiple organ retardation.
2. After DENV-2 infection, placental vasculature is seriously damaged in mice and placental samples from pregnant women also show comparable histological alterations.
3. Single-cell RNA sequencing reveals that neutrophils play key roles in placental histopathology damage after DENV-2 infection. Neutrophil elastase inhibitor can effectively mitigate the harm of placental vasculature and fetal growth restriction caused by DENV-2 infection in our mouse model.

### Implications of all the available evidence

Placental immunopathological changes, rather than the viral transplacental transmission, are linked to fetal intrauterine growth restriction caused by DENV-2 infection, indicating that alleviating the destructive effect of neutrophil infiltration represents a feasible therapeutic strategy.

## Introduction

Dengue virus (DENV) belongs to the *Flavivirus* genus of *Flaviviridae* and is transmitted through the bites of the mosquitos *Aedes aegypti* and *Aedes albopictus*. There are four distinct but closely related serotypes (DENV-1, DENV-2, DENV-3, and DENV-4). DENV is still a major public health issue, particularly in tropical and subtropical regions worldwide. It was estimated that over 2.5 billion people live in places where dengue infection is a serious health threat[1] and that approximately 390 million people are infected with DENV each year, with approximately 96 million showing obvious clinical symptoms and requiring hospitalization. In 2019, the WHO declared dengue one of the top 10 global health threats.

DENV infection has progressively achieved the status of a pandemic, and pregnant women are among the high-risk populations. Recently, an increasing number of cases of DENV infection during pregnancy have been reported and are definitely associated with increased morbidity and mortality in both mothers and fetuses.[2–4] Meta-analysis showed that preterm birth and low birth weight are the most common adverse pregnancy outcomes associated with maternal DENV infection.[5,6] Further histopathological examinations of placentas collected at delivery from maternal DENV infection have shown hypoxic lesions with villous stromal edema and infarcted and preinfarcted areas in 19 of 24 cases, including eight from mothers who did not report overt shock syndrome.[7] DENV infection can impose deleterious effects on the placenta and, consequently, on fetal growth/development.[8] Most of the reports on adverse pregnancy outcomes associated with maternal DENV infection thus far have focused on clinical phenotypic analysis, but the underlying mechanism generating fetal complications remains poorly understood.

During pregnancy, several mechanical and physiological changes in the mother are required to accommodate the fetus.[9] The maintenance of a successful pregnancy requires good development of a functional placenta, which forms a crucial physical barrier between the maternal and fetal compartments, preventing pathogen transmission during pregnancy. In terms of histomorphology, both mouse and human placentas have hemochorial systems.[10,11] The human placenta is mainly composed of extravillous cytotrophoblasts, column cytotrophoblasts, and chorionic villi, while the mouse placenta is mainly composed of trophoblast giant cells, spongiotrophoblasts and the labyrinth. In both species, maternal blood enters the placenta from the uterine arteries to the spiral arteries located in the maternal decidua. The maternal blood then percolates through a dense mesh of channels created and lined by fetal trophoblast cells, inside which an equally dense network of fetal capillaries is localized. This area, known as the villous tree in humans, is a critical location of feto-maternal exchange of gases, nutrients, and metabolites, while the labyrinth in mice performs such functions.[11] It is suggested that mice are a useful alternative model for studying pregnancy diseases associated with placental dysfunction.[12]

The establishment and maintenance of pregnancy requires degradation and remodeling of the extracellular matrix (ECM) to allow placental vasculature. In this process, neutrophils play an important role. On the one hand, neutrophils release specific proteases such as matrix metalloproteinases (MMPs) to tightly regulate the degradation of ECM[13,14] and promote neovascularization. On the other hand, deregulated or aberrant activation of neutrophils may be associated with placental tissue damage and even the development of complex pregnancy-related disorders.[13,15] The

mechanisms whereby DENV infection could lead to adverse pregnancy outcomes are unknown, but whether DENV infection causes placental immunopathological damage and hemodynamic changes or DENV has a direct effect on the fetus[16–19] needs further exploration.

Here, *Ifnar1*$^{-/-}$ mice, a well-known mouse model in the field of flavivirus research,[20,21] were used to investigate the effects of DENV-2 infection on the growth of fetuses, pregnancy outcomes, placental histopathological features and inflammatory cell infiltration and the associated mechanism underlying this process in a mouse model. The changes in placental cell populations were also profiled by exploiting single-cell RNA-seq methodology. Zika virus (ZIKV), another important *Flavivirus*, has been widely reported to be associated with a range of adverse pregnancy complications, including microcephaly, IUGR, spontaneous abortion, and stillbirth,[22] and was used as a positive control in this study. Our findings will provide important experimental evidence for clarifying the pathogenesis of adverse pregnancy outcomes caused by DENV infection and a theoretical basis for further clinical research.

## Methods

### Ethics statement

All procedures with animals were undertaken according to the Institutional Animal Care and the Animal Ethics Committees of Capital Medical University, Beijing, China. Patients provided written consent for the use of deidentified and discarded tissues for research purposes upon admission to the hospital.

### Mice, cells, and viruses

C57BL/6 mice deficient in interferon α/β receptors (*Ifnar1*$^{-/-}$ mice) were purchased from the Institute of Zoology, Chinese Academy of Sciences, and were bred on an automatic light cycle (12 h light:12 h dark) in a specific pathogen-free facility. For pregnancy establishment, eight-to ten-week-old female *Ifnar1*$^{-/-}$ mice were cohabited with male *Ifnar1*$^{-/-}$ mice at a ratio of 2:1. The female mice were examined for vaginal plugs the next morning, and then the male mice were removed from the cage. The sample size of pregnant mice used in this study was further verified by "resource equation" method based on law of diminishing return.[23] After evaluation, the values of "E" all lied between 10 and 20 excluding the experiment involving in screening possibly changed factors. The body weight was monitored throughout pregnancy. For viral infection, pregnant *Ifnar1*$^{-/-}$ mice were challenged with $10^5$ PFU DENV-2 or $10^4$ PFU ZIKV at E12.5 (embryonic day 12.5) through footpad injection, and an equal volume (100 μL) of phosphate-buffered saline (PBS) was used as a control. Treatments were randomly allocated to the experimental units entirely at random. After infection, the symptoms were recorded daily until 6 dpi. The mice were euthanized at 6 dpi, and the conceptuses, amniotic fluid, maternal blood, and major organs were collected for subsequent experiments, e.g., the determination of viral loads, cytokine levels or histological examination. For sivelestat injection, pregnant mice were injected with PBS or sivelestat (100 mg kg$^{-1}$ i.p., dissolved in PBS) at E12.5. Sivelestat (ONO-5046) was purchased from AbMole Bioscience (USA).

The human choriocarcinoma cell line BeWo, a well-characterized cell model of human placental trophoblasts, was cultured in Ham's F12K media (Kaighn's; Gibco) supplemented with 10% FBS. DENV-2 (strain Tr1751) was kindly provided by Dr. Kotaro Yasui[24,25] and was then stored in our laboratory. ZIKV (strain SMGC-1, Asian lineage, GenBank accession number: KX266255) was isolated from an imported case returning to China from Fiji at Shenzhen Port and provided by Dr. George Fu Gao.[26,27] For DENV-2 and ZIKV production, the *Aedes albopictus* mosquito cell line (C6/36) was cultured in RPMI-1640 medium supplemented with 10% fetal bovine serum (FBS; Gibco, USA) or with 2% FBS for viral propagation and passage. The titers of infectious virus were determined by a plaque formation assay on a monolayer of Vero cells. Vero cells were maintained in minimum essential medium (MEM) supplemented with 5% FBS and were overlaid with medium containing 1.2% methylcellulose when conducting a plaque assay to detect viral titers.

### Human samples

The placental sections from three healthy pregnant women and two pregnant women infected with DENV in the third trimester were harvested. The two groups were matched according to age, gravidity and parity history, date of delivery, and outcome of the mother and the fetus (Supplemental Table S1). In view of limited sample size, only descriptions of histomorphology changes were provided in this study, and statistical comparison was not available. DENV infection was confirmed in the third trimester (38 weeks plus five days and 38 weeks plus one day) by positive detection in serum of DENV NS1 antigen, DENV RNA and typical dengue symptoms including fever, headache, arthralgia, rash, or hepatic insufficiency. Both the uninfected and DENV-infected cases had no underlying disease, and all the neonates were delivered with no clinical symptoms. The placentas were obtained after parturition at term. Placental biopsies and placental sections used in this study were prepared according to the standard operating procedure of the clinical pathological laboratory. In brief, after delivery, weighing, measurement, and observation, placenta samples were randomly and extensively harvested from four distinct sites: the cord insertion site, midway between the cord insertion and the periphery of the placenta, which included both the maternal and fetal sides, and the outer disks as well as any other sites.

### Colorimetric assay and ELISA

The amniotic fluid in the mouse experiments was harvested from conceptuses by suction and stored at –80 °C until analysis. Colorimetric assay kits were used to quantify the concentrations of phosphatidylcholine (BioVision, USA), sphingomyelin (BioVision, USA), creatinine (NJJCBIO, China), and amylase (NJJCBIO, China) in amniotic fluid according to the manufacturer's instructions. Briefly, the standards, blanks, and prediluted samples were added to a 96-well plate, followed by the addition of Reaction Mix. After incubation, the light absorbance was read at the proper wavelength on a Multiskan Spectrum 1500 (Thermo Scientific, USA). Sample readings were applied to the standard curve, and the concentrations of the test samples were then calculated. The levels of progesterone (Cloud-Clone, USA), estradiol (Cloud-Clone, USA), beta-chorionic gonadotropin (MEIMIAN, China), prolactin (MEIMIAN, China), and placental growth factor (Cloud-Clone, USA) in serum were detected by ELISA kits according to the manufacturer's protocols.

### Quantitative inflammation array

Maternal blood was harvested by lancing the facial vein, and then serum was collected from the supernatant. The placentas were snap-frozen in liquid nitrogen once separated from pregnant *Ifnar1*$^{-/-}$ mice. The concentrations of 40 cytokines in serum and placental extracts were determined using the Quantibody Mouse Inflammation Array Kit according to the manufacturer's instructions (RayBiotech, USA). Quantitative array analysis was performed using RayBiotech data processing software (QAM-INF-1_Q-Analyzer). The concentrations of various cytokines in the placenta were adjusted by organ weight and expressed as picograms per milligram of tissue.

### Doppler ultrasound imaging

At 5 dpi (E17.5), the pregnant mice were placed in the supine position on a heated platform under 1.5% isoflurane anesthesia. The abdominal fur was removed with a depilatory cream. The blood flow of the umbilical cord and placenta was evaluated using a high-frequency ultrasound system (Vevo2100, VisualSonics, Canada).

### Hematoxylin and eosin staining

The placentas isolated from infected or uninfected mice were fixed in 4% paraformaldehyde overnight and then embedded in paraffin blocks using an automated tissue processor (Leica, Germany). After sections (5-μm thickness) were prepared, deparaffinized, and rehydrated, hematoxylin and eosin were used to stain the sections to observe histomorphology.

### Immunohistochemistry (IHC) staining

To assess placental vasculature damage and immunocyte infiltration after infection, the sections were incubated with a rabbit anti-CD34 antibody (1:600, Abcam, ab81289) or a rabbit anti-Ly6g antibody (1:1750, ab238132, Abcam) at 4 °C overnight. A secondary HRP-conjugated goat anti-rabbit antibody (PV-9001, ZSGB-BIO) was used to stain the slides. To visualize the reaction, the chromogen 3,30-diaminobenzidine (DAB, ZLI-9018, ZSGB-BIO) was added to the slides, followed by washing with running water. The sections were then stained with hematoxylin to mark the nucleus. Placental vascular parameters (vessel density, branch points, and end points density) were analyzed in the labyrinth zone using AngioTool.[28]

### Wright-Giemsa staining

Maternal and fetal blood smears were prepared and air dried naturally. Wright-Giemsa solution (SolarBio, G1020, China) was subsequently added to cover the entire specimen smear, followed by incubation at room temperature for 2 min. Phosphate buffer (pH 6.4) was added, and the smear was gently shaken to mix with the Wright-Giemsa solution thoroughly. After dyeing for 3–5 min, the solution was discarded, followed by washing in water. The morphology of erythrocytes was observed under an Olympus BX61 microscope.

### Western blotting

Placentas were homogenized and lysed in RIPA buffer containing a protease and phosphatase inhibitor cocktail (Thermo Scientific). Equal amounts of lysates (10 μL) were separated using SDS–PAGE gels and transferred onto PVDF membranes (GE Healthcare, USA). After the membranes were blocked with TBST buffer containing 10% skim milk, primary antibodies against MMP-2 (1:500, Invitrogen, PA5-117,038), MMP-8 (1:500, Abcam, ab53017), MMP-9 (1:1000, Abcam, ab38898), MMP-12 (1:1000, Invitrogen, MA5-32011), MMP-25 (1:1000, Invitrogen, PA5-109967), TIMP-1 (1:500, Invitrogen, MA1-773), TIMP-2 (1:500, Invitrogen, MA1-774) or GAPDH (1:1000, Cell Signaling Technology, 5174S) were added and incubated with the membranes overnight at 4 °C. The next day, the membranes were washed with TBST three times, followed by incubation with a goat anti-rabbit secondary antibody (1:5000, LI-COR, 926-68071) or a donkey anti-mouse secondary antibody (1:5000, LI-COR, 925-32212). Band intensities were visualized and quantified using an infrared laser imager (Odyssey® CLX, USA) and normalized to the housekeeping control protein (GAPDH) expression. The information about antibodies and main reagents used in this study were provided in Supplemental Table S2.

### Transcriptome sequencing

Placentas isolated from pregnant mice were homogenized in TRIzol, and total RNA was extracted according to the manufacturer's instructions. The purity and concentration of RNA were verified by a NanoPhotometer. The RNA integrity was assessed by electrophoresis (1%

agarose gels) using an Agilent 2100 bioanalyzer. The sequencing libraries were obtained using the NEBNext Ultra RNA Library Prep Kit for Illumina (NEB, USA) and sequenced on an Illumina NovaSeq platform, and 150-bp paired-end reads were generated. Clean reads were generated by removing reads containing adapters and poly-N and reads of low quality. After trimming, the clean reads were mapped back to the reference genome (GRCm38.p6) using Hisat2 software (version 2.0.5), and the gene expression levels were quantified by the expected number of fragments per kilobase of transcript sequence per million base pairs sequenced (FPKM). A differential expression analysis between the DENV-infected group and the uninfected group was performed using the DESeq2 R package (Version 1.16.1). The original p values were adjusted by Benjamini and Hochberg's approach to control the false discovery rate, and only genes with an adjusted p value (adj-p) < 0.05 and $|\log_2$ (fold change) | > 0 were deemed differentially expressed genes (DEGs). The DEGs were then subjected to Gene Ontology (GO) enrichment and Kyoto Encyclopedia of Genes and Genomes (KEGG) pathway analyses.

### Single-cell RNA sequencing (scRNA-seq)

The placentas from DENV-infected or uninfected *Ifnar1*$^{-/-}$ mice were transferred into MACS C-tubes (Miltenyi Biotec). After dissociation, filtering, centrifugation, and resuspension, single-cell suspensions excluding erythrocytes and cell debris were obtained. The overall cell viability was confirmed to be above 85% using the trypan blue exclusion method. The concentration of single-cell suspensions was detected by an automated cell counter and adjusted to 700–1200 cells/μL. A Chromium Controller (10× Genomics) was used to capture single cells by microfluidic technology according to the manufacturer's instructions (LC-Bio Technology, China). After the cDNA amplification and library construction steps were performed, an Illumina sequencing platform (NovaSeq 6000) was used to detect the cDNA library. Cell Ranger software was used to demultiplex samples, process barcodes, and quantify single-cell 3′ genes. The scRNA-seq data were then aligned to the Ensembl genome GRCm38 reference genome, and Seurat (version 3.1.1) was used for further dimensional reduction, clustering, and analysis. Through detailed analysis of complex cell populations, single-cell expression maps were drawn, and gene expression profiles at the single-cell level were obtained.

### RT-qPCR

Pregnant *Ifnar1*$^{-/-}$ mice were euthanized at the indicated times. Maternal blood, spleen, liver, fetuses and their corresponding placentas, amniotic fluid, and major organs were collected. Tissues stored at −80 °C were homogenized, and total RNA was extracted using TRIzol (Sigma, USA) according to the manufacturer's protocol. The levels of viral RNA and mRNA transcripts for MMPs were determined by a Quant One Step RT–qPCR Kit (SYBR Green, TIANGEN, China) in a 7500 Real Time PCR System (Applied Biosystems, USA). Viral RNA copies were normalized by a standard curve as we previously published.[29] Viral loads are expressed on a $\log_{10}$ scale as copy number per gram of tissue or per milliliter of blood. The primer sets for MMP genes were from reported methods (Supplemental Table S3).[30–35] The specificity of these primer sets has been aligned in NCBI, and the PCR amplification products were electrophoresed and sequenced. Relative mRNA levels were calculated using the standard method and GAPDH as an endogenous reference gene.

### Quantification and statistical analysis

Data visualization and statistical analyses were performed in GraphPad_Prism_7.0. The normality of the datasets was determined by the Kolmogorov–Smirnov test. The data with normal distributions were analyzed by ordinary one-way ANOVA followed by Tukey's multiple comparison test (Fig. 1b, Fig. 2, Fig. 3d, Fig. 4c, Fig. 5c, Fig. 7b and e) or Bonferroni's multiple comparison test (Fig. 1d and f, Fig. 4e, Fig. 5a, Fig.7b, Supplemental Figure S2b). Data are presented as the mean ± standard deviation (SD) or mean ± standard error of the mean (SEM). Comparisons were considered significantly different when $p < 0.05$.

### Role of funders

The funding authorities did not play any role in study design, data collection, data analyses, interpretation, or writing of report.

## Results

### DENV-2 infection causes fetal growth restriction in pregnant *Ifnar1*$^{-/-}$ mice

To mimic the course of DENV infection during late pregnancy and to determine the effect on fetuses, pregnant *Ifnar1*$^{-/-}$ mice on E12.5 were challenged with $10^5$ PFU DENV-2 or $10^4$ PFU ZIKV (Fig. 1a). The infection course and body weight of mice were monitored. The blood and major organs of pregnant dams, placentas, and fetal tissues were harvested on E18.5. The results showed that the body weight of uninfected mice continuously increased, but the rate of weight increase in DENV-2- or ZIKV-infected mice appeared to slow down at 3 days after infection (dpi) and then began to decrease at 5 dpi (E17.5) (Supplemental Figure S1a). Compared with the uninfected group, after DENV-2 infection, the pregnant mice displayed pilomotor fur and slow movement at 3 dpi, followed by progressively deteriorating conditions, which were worse than those of ZIKV-infected mice (Supplemental Figure S1b). No deaths were observed in either group during our observation period. These results suggested that pregnant *Ifnar1*$^{-/-}$ mice are susceptible to both virus strains.

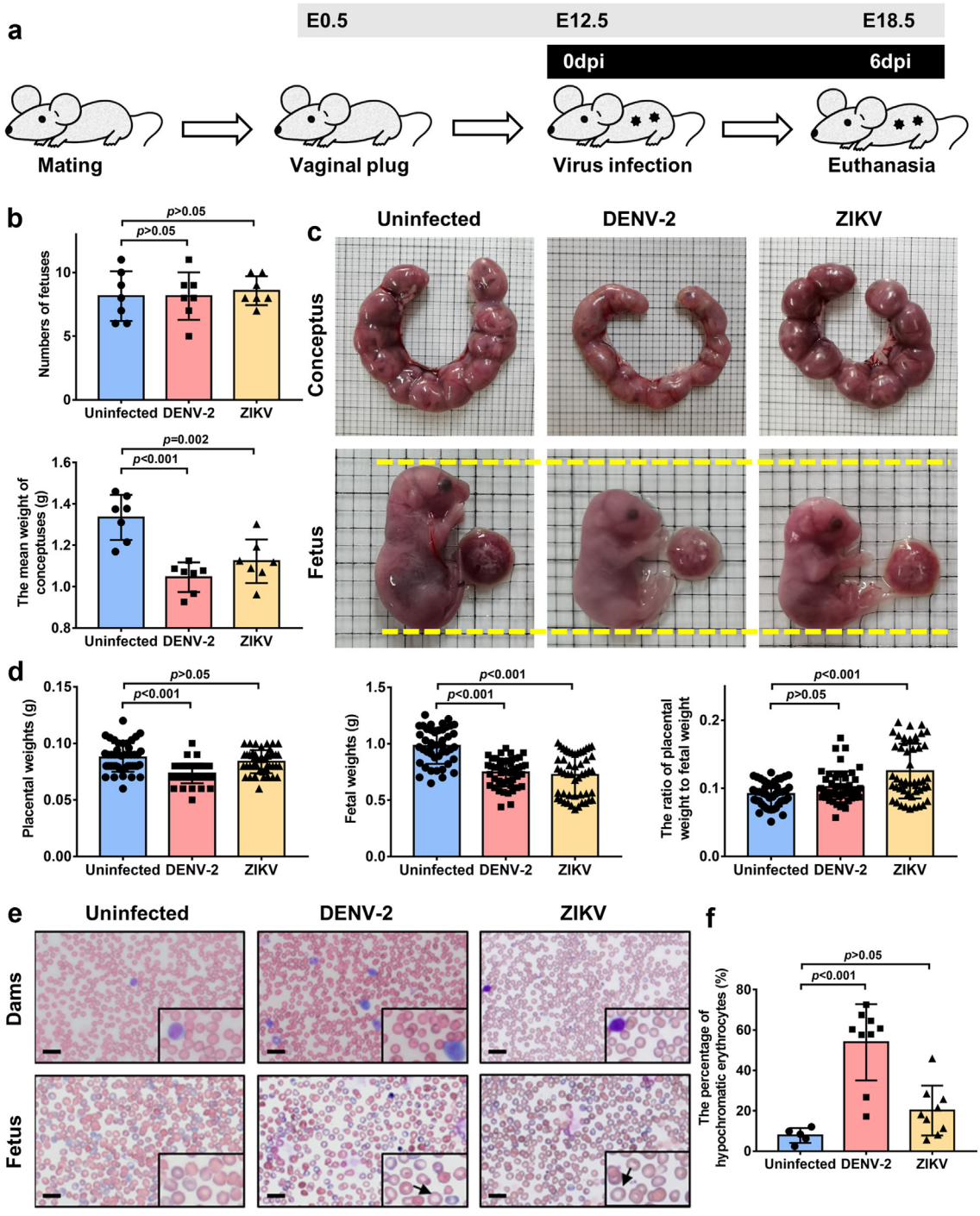


***Fig. 1:*** **DENV-2 and ZIKV infection leads to fetal intrauterine growth restriction in *Ifnar1*$^{-/-}$ mice.** (a) Schematic diagram of the viral infection model during pregnancy. Pregnant dams were subcutaneously inoculated with $10^5$ PFU DENV-2 or $10^4$ PFU ZIKV on E12.5. Mice were sacrificed at 6 days post infection (dpi) and the maternal blood and conceptuses were collected. (b) The numbers of fetuses and the mean weights of conceptuses of uninfected dams, DENV-2-infected dams, or ZIKV-infected dams were evaluated. N = 7 per group. (c) Representative images of E18.5 uteri, fetuses, and placentas from uninfected, DENV-2-infected and ZIKV-infected mice respectively, the latter two of which exhibited growth restriction. (d) The changes of placental weights, fetal weights were evaluated. The ratio of placental weight to fetal weight among three groups were measured to reflect the coordination of placental and fetal development. Uninfected mice were considered as controls. Each spot represents an individual fetus. N = 44 in the uninfected group, N = 49 in the infected groups. Fetuses in each group were

At 6 dpi (E18.5), the pregnant mice were sacrificed, and the fetuses were collected. We found that the number of fetuses in DENV-2- and ZIKV-infected mice was comparable to that in uninfected mice. However, after DENV-2 infection, the mean weight of the conceptus (the ratio of the total weight of the conceptus to the number of fetuses) was robustly lower and the body length of the fetuses was smaller than those of the uninfected group (Fig. 1b and c). Surprisingly, gross examination of the fetuses and placentas revealed hypoperfusion manifested by pale appearance (Fig. 1c). The above results were also observed in the ZIKV-infected group. We then compared the differences in placental and fetal weights among the above three groups. Unlike the uninfected group, both the placental and fetal weights in DENV-2 pregnant mice decreased significantly (Fig. 1d), suggesting that DENV infection could cause insufficient nutrient supply to the fetuses. In other words, the mouse model of adverse pregnancy induced by DENV infection was successfully established. In ZIKV-infected pregnant mice, the fetal weight distinctly decreased, but the placental weight was unchanged (Fig. 1d). The ratio of placental weight to fetal weight was measured to reflect the coordination of their development.[36,37] The results showed that the ratio in ZIKV-infected mice was increased (Fig. 1d), indicating that ZIKV infection could cause unbalanced development between placentas and fetuses.

To verify whether DENV infection in pregnant dams affects fetal nutritional deficiency, we observed the morphology of maternal and fetal erythrocytes by Wright-Giemsa staining. The results revealed that DENV-2 infection did not affect the morphology and number of maternal erythrocytes, but the number of fetal poikilocytes and hypochromic erythrocytes manifested by an enlarged central light staining area substantially increased. A similar manifestation was also observed in the ZIKV-infected group (Fig. 1e and f). These results suggested that DENV-2 or ZIKV infection in pregnant mice led to anemia in fetal mice. In combination with the shorter body length of the fetuses, these results further indicated that maternal DENV-2 or ZIKV infection could cause fetal growth restriction.

To further clarify the characteristics of intrauterine growth restriction (IUGR) caused by maternal DENV-2 or ZIKV infection, we then measured the levels of phosphatidylcholine, sphingomyelin, creatinine, and amylase in amniotic fluid. The levels of phosphatidylcholine and sphingomyelin and their ratio can prominently reflect the maturity of the fetal lung; the levels of creatinine and amylase are typical test indicators that reflect the maturity of the fetal kidney and pancreas, respectively.[38–40] After DENV-2 or ZIKV infection, the levels of phosphatidylcholine, creatinine and amylase decreased significantly, indicating retardation of the fetal lung, kidney, and pancreas. No overt difference was observed in the levels of sphingomyelin between the uninfected group and the infected groups. Thus, the ratio of phosphatidylcholine to sphingomyelin in the infected groups also decreased (Fig. 2). These results further indicated that DENV-2 and ZIKV infection in our pregnant mouse model could lead to fetal dysmaturity manifested by multisystem retardation.

### Vertical transmission was not observed in the DENV-infected mouse model

To explore whether DENV-2 infects the fetus through transplacental vertical transmission, the distribution of DENV antigen in the placenta and the DENV RNA level were detected. DENV antigen was mainly observed in the cytoplasm of leukocytes and the vascular endothelium in the placental labyrinth and giant trophoblast layer (Fig. 3a). DENV-2 RNA levels ranging from $10^8$ to $10^{12}$ copies per gram or milliliter were detected in maternal blood (7/8), spleen (6/6), liver (3/7) and placenta (7/7) at 6 dpi. There was no detectable viral RNA in any amniotic fluid, fetal brain, or liver. Notably, unlike in the DENV-2-infected group, ZIKV RNA was detectable not only in maternal blood, major organs, and placenta but also in amniotic fluid (7/9), fetal brain (8/8) and fetal liver (7/8) (Fig. 3b). These results indicated that in our mouse model, ZIKV could infect fetuses through transplacental transmission, but DENV-2 could not.

Placental trophoblast cells are an important part of the blood-placental barrier that defend against virus infection.[41] It is reported that ZIKV can infect placental trophoblast cells and endothelial cells.[42,43] To explore the mechanism underlying the difference in transplacental transmission between DENV-2 and ZIKV, BeWo cells, a human choriocarcinoma cell line, were infected with DENV-2 or ZIKV at a multiplicity of infection (MOI) of 1. We found that ZIKV could infect approximately 40% of BeWo cells at 24 h post-infection, but few cells were infected by DENV-2 (Fig. 3c and d). The above results indicated that ZIKV could achieve transplacental transmission by infecting trophoblast cells; however, in contrast to ZIKV infection, DENV-2 could not infect fetuses through

carried by 6 pregnant dams. (e) Representative images of Wright-Giemsa staining of maternal and fetal blood smears in uninfected group and infected groups. The images with higher magnification are displayed as inserts. Hypochromic erythrocytes indicated fetal anemia, showed by arrows. Scale bar = 10 μm. (f) The percentages of hypochromic erythrocytes of fetal blood were analyzed. Each spot represents an individual fetus. N = 5 in the uninfected group from 3 dams, N = 9 in the infected groups from 4 dams. Data are presented as the mean ± SD (b, d, and f). The significance of differences was analyzed by one-way ANOVA with a Tukey's multiple comparison test (b) or a Bonferroni's multiple comparison test (d and f).

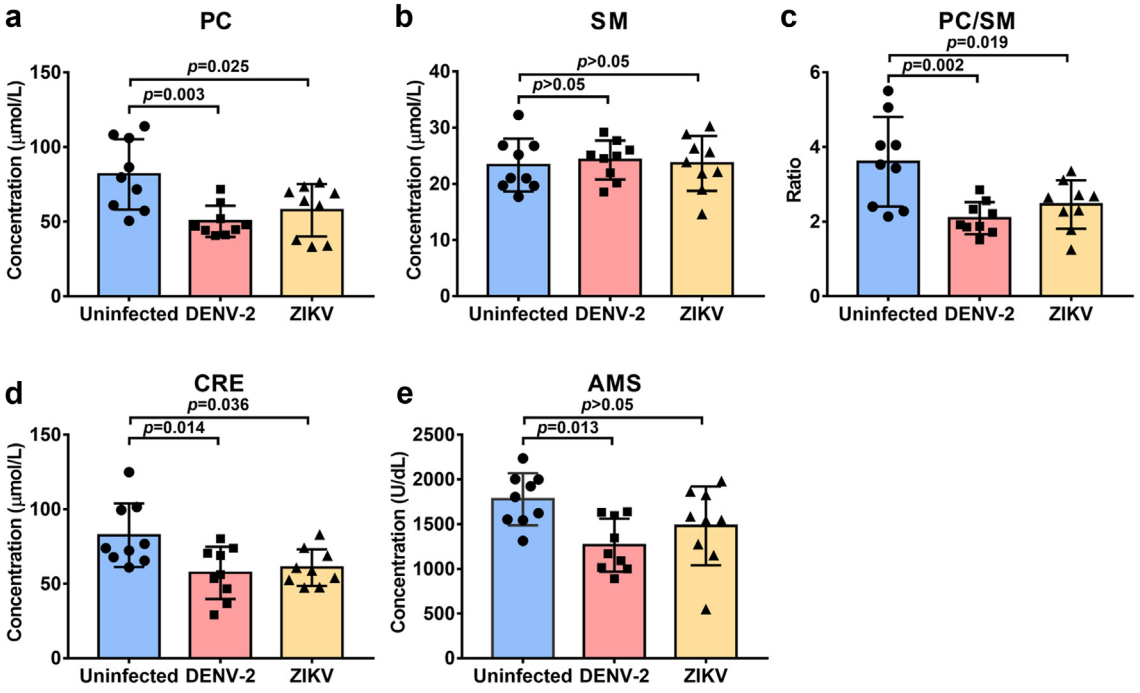


***Fig. 2:* The detection of biochemic markers in amniotic fluid reflecting the maturity of fetal organs.** The levels of phosphatidylcholine (a), sphingomyelin (b), the ratio of phosphatidylcholine to sphingomyelin (c), creatinine (d), and amylase (e) in amniotic fluid were determined by colorimetric assay kits to reflect the maturity of fetal major organs. Phosphatidylcholine: PC, sphingomyelin: SM, creatinine: CRE, amylase: AMS. N = 9 per group. Data are presented as the mean ± SD. The significance of differences was analyzed by ordinary one-way ANOVA with a Tukey's multiple comparisons test.

transplacental transmission in this mouse model, suggesting that fetal growth restriction caused by DENV-2 infection may not be attributed to direct damage by viral replication within the fetuses and that other key factors may be involved in the process.

### Fetal IUGR may result from placental vasculature damage and hypoperfusion in DENV-2-infected pregnant *Ifnar1*$^{-/-}$ dams

Histopathological changes in the placenta induced by DENV-2 infection were investigated by hematoxylin and eosin (H&E) staining. In the uninfected group, the trophoblast giant cells were clearly visible. The labyrinth appeared to have denser cellularity, and the blood vessels in this area were full of erythrocytes. In contrast, degeneration of trophoblast giant cells and focal necrosis were observed in the junctional zone after DENV-2 infection. The most prominent change was the disorganized and unfilled vasculature in the labyrinth zone (Fig. 4a).

Tissue sections of E18.5 placentas were immunohistochemically stained with an antibody against CD34 to label microvessels.[44] Compared with the uninfected group, the placental vasculature in the labyrinth layer was unevenly distributed and partially collapsed, and most of the vascular luminal spaces almost disappeared in the DENV-2-infected group (Fig. 4b, left panel). AngioTool software was then used for the analysis of vascular characteristics in the labyrinth zone.[28] The results showed that the vascular density and the number of branch points were decreased significantly after DENV-2 infection (Fig. 4b, right panel, and Fig. 4c), which was also observed in ZIKV-infected placentas. Accordingly, the mean lacunarity, which reflected inhomogeneity of vascular distribution, was obviously increased after DENV-2 or ZIKV infection. These results indicated that defective development of the placental vasculature in the labyrinth may precede fetal growth restriction following DENV-2 infection of pregnant dams.

Next, color Doppler ultrasound imaging technology was used to monitor the real-time dynamics of placental blood flow at 5 dpi (E17.5), the day before harvest. In the uninfected group, the placental blood supply was sufficient, and vascular branches were clearly observed. However, after DENV-2 infection, the placental vascular branches almost disappeared (Fig. 4d), and the peak systolic velocity (PSV), end diastolic velocity (EDV) and mean velocity (MV) of placental blood flow decreased significantly. In addition, the values of the velocity time integral (VTI), pulsatility index (PI) and resistance index (RI) did not change significantly in the DENV-2-infected

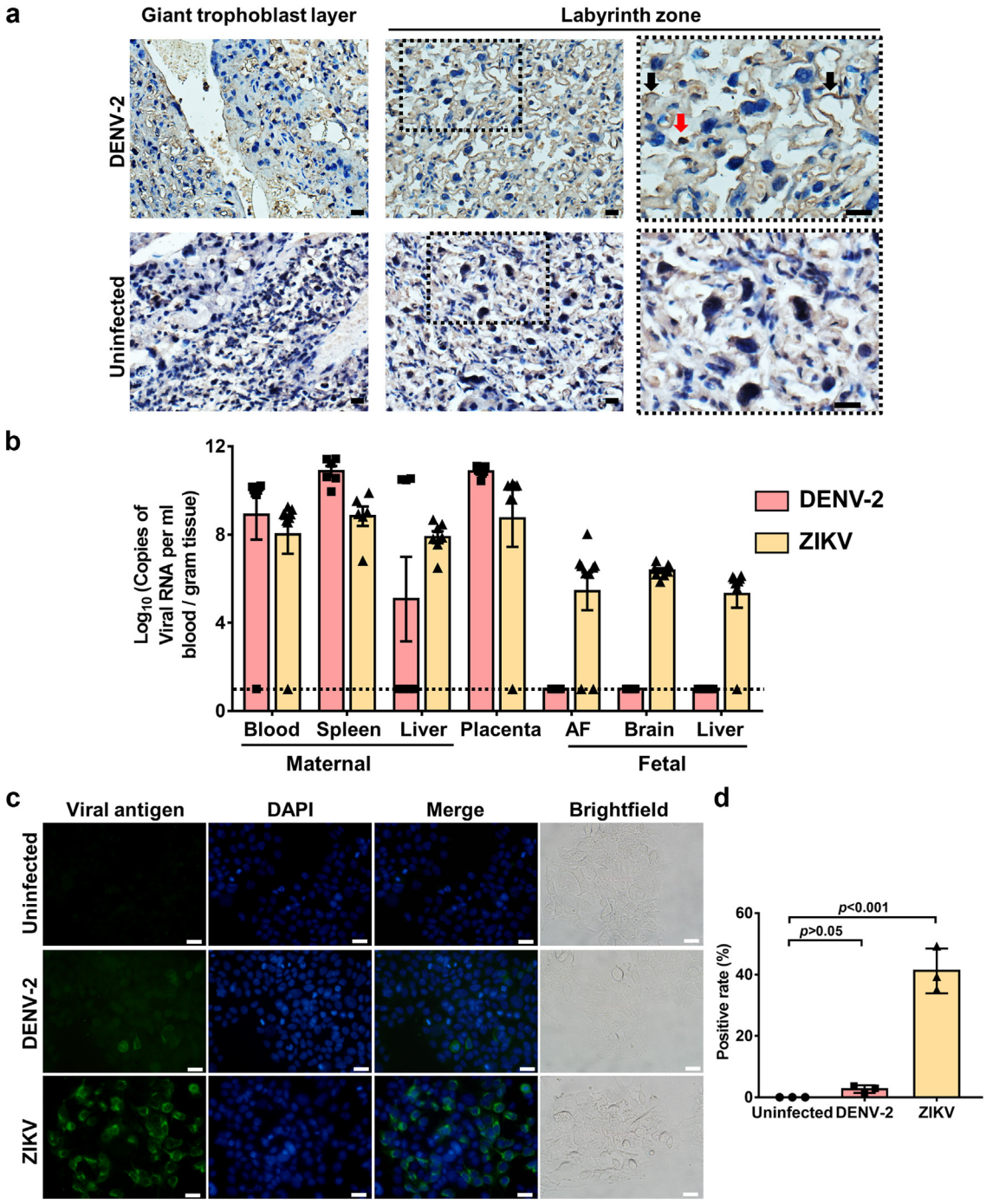


***Fig. 3:* The comparison of transplacental transmitting capacity of DENV-2 and ZIKV.** (a) The distributions of DENV-2 in the placentas at 6 dpi were detected by IHC. Uninfected placentas served as controls. Red and black arrow indicated positive DENV-2 antigen staining. Scale bar = 20 μm. (b) The viral burden in the maternal blood, spleen, liver, placentas, and fetal amniotic fluid, brain, and liver at 6 dpi were measured by RT-qPCR, N = 6 - 9 per group. The dotted line indicates the limit of detection. (c) Representative immunofluorescence images of BeWo cells infected with DENV-2 or ZIKV at MOI = 1 for 24 h. Uninfected BeWo cells were considered as controls. Virus-positive cells are shown in green and DAPI staining of nuclei is shown in blue. The right one panel is representative images of brightfield microscopy. Scale bar = 20 μm. (d) Percentages of BeWo cells infected with DENV-2 or ZIKV at MOI = 1 for 24 h were evaluated and the data were from three independent experiments. Data are presented as the mean ± SEM (b) mean ± SD (d). The significance of differences was analyzed by ordinary one-way ANOVA with a Tukey's multiple comparisons test (d).

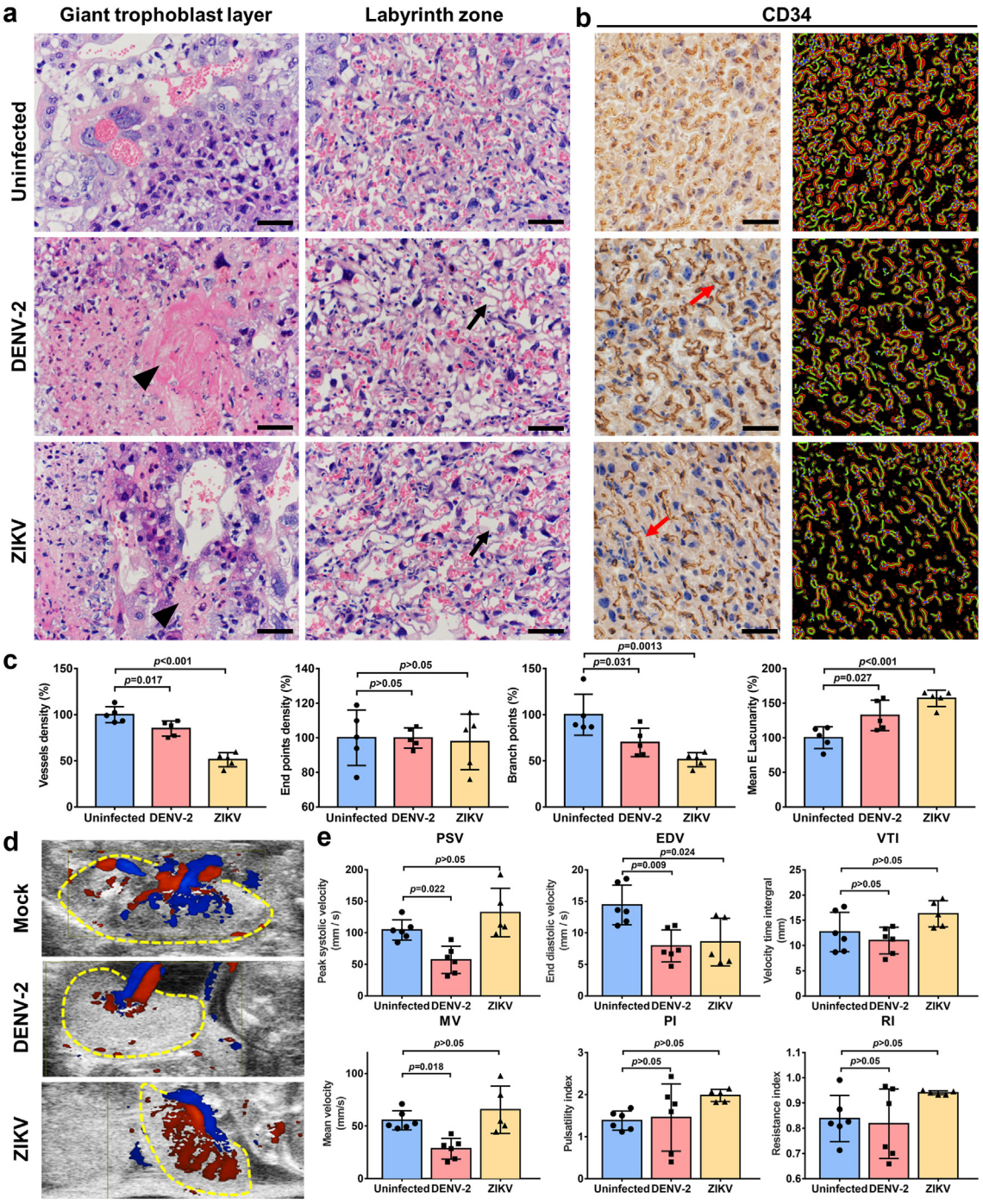


***Fig. 4:*** **Changes of histopathology and blood flow in the placentas after infection.** Pregnant dams were subcutaneously inoculated with $10^5$ PFU DENV-2 or $10^4$ PFU ZIKV on E12.5. The blood flow of placenta was monitored at 5 dpi. The placentas were collected at 6 dpi. (a) Histopathological changes were analyzed by HE staining. Scale bar = 100 μm. Arrowhead, focal necrosis; arrow, unfilled vessel. (b) CD34 expression in placental labyrinth zone was assessed by IHC staining at 6dpi. Uninfected placentas were considered as controls. Red arrow, collapsed vessel. CD34-positive microvessels were visualized by AngioTool software. The red areas outlined placental microvessels, the green lines indicated the direction of the vessels, and the blue dots indicated the branch points of the vessels. Scale bar = 100 μm. (c) Quantification of vessel density, end point density, branch points, and mean lacunarity in placental labyrinth zone. N = 5 per group. (d) Examination of blood flow of uninfected, DENV-2-infected or ZIKV-infected placentas by using a doppler ultrasound system. The blue colors and red colors indicated the

group (Fig. 4e). After ZIKV infection, only EDV decreased obviously whereas other indicators did not alter significantly. These results suggested that DENV-2 infection could cause placental vascular damage and severe insufficient perfusion, thereby exhibiting hemodynamic changes.

The pregnant mice were then injected with 100 μL of Evans Blue at 6 dpi (E18.5). We found that the dye was mainly present in the placenta and was undetectable in the amniotic fluid and fetuses in the uninfected or infected groups (Supplemental Figure S2a), suggesting the relative integrity of the maternal–fetal barrier.

Next, the hormones responsible for maintaining pregnancy were measured with ELISA. The results revealed that the levels of these hormones did not obviously change after DENV-2 or ZIKV infection (Supplemental Figure S2b), indicating a limited influence of the viruses on placental endocrine function.

### Abnormal degradation of the extracellular matrix causes damage to the placental vasculature

Based on the above findings of abnormal vasculature in the placental labyrinth, differential expression of genes in DENV-2-infected placentas was analyzed by RNA sequencing. The results revealed that after DENV-2 infection, 430 genes were upregulated, and 410 genes were downregulated. According to GO cluster analysis, the most significant changes were in the pathways of defense response, extracellular matrix, and epithelial tube morphogenesis (Supplemental Figure S3), suggesting that DENV-2 infection could seriously impair placental angiogenesis. According to Reactome cluster analysis, we also found that the pathway of extracellular matrix organization was largely modulated by DENV-2 infection, with 13 genes significantly upregulated and 16 genes downregulated (Supplemental Figure S4a and b).

Matrix metalloproteinases (MMPs) play an important role in placental vascular remodeling.[45] Among the differentially expressed genes in extracellular matrix organization, MMPs, including MMP-8, MMP-25, and MMP-9, were markedly upregulated (Supplemental Figure S4c). MMPs are known to degrade the components of the extracellular matrix, such as collagen and gelatin, to regulate vascularization.[46,47] Tissue inhibitors of matrix metalloproteinase (TIMPs) are responsible for inhibiting the activity of MMPs, and major functional components include TIMP-1 and TIMP-2.[48,49] The expression of MMPs and TIMPs at the mRNA and protein levels was assessed by RT−qPCR and WB, respectively. Notably, the expression levels of MMP-2 and MMP-12 genes were decreased, while the MMP-8, MMP-9 and MMP-25 gene levels were increased after DENV-2 infection, although TIMPs did not change significantly (Fig. 5a). At the protein level, MMP-12 was downregulated, and MMP-9 was upregulated. However, the expression levels of other MMPs did not change significantly. After DENV-2 infection, the expression level of TIMP-2 protein was obviously increased, while TIMP-1 did not change significantly (Fig. 5b and c). Similar change trends in the protein levels of placental MMPs were also observed in ZIKV infection. These results suggest an important role for MMPs in mediating damage to the vasculature in the labyrinth during maternal DENV-2 infection as an underlying mechanism of placental dysfunction.

### Abnormal expression of MMPs induced by DENV-2 infection can be attributed to neutrophil infiltration into the placenta

Next, the cytokine and chemokine profiles in the serum of pregnant mice and placenta were detected with a mouse inflammation array. Compared with uninfected mice, the levels of G-CSF, IFN-γ, Eotaxin, MIG, RANTES, MCP-1, and MCP-5 in serum were distinctly increased. Surprisingly, the levels of granulocyte chemokines in the placentas, including G-CSF, PF4, IL-1a, and KC (CXCL1),[50–53] were significantly increased (Fig. 6a). Correspondingly, we found that the levels of molecules related to the interaction of granulocytes with endothelial cells, such as ICAM-1 and TIMP-1,[13,54] were also significantly increased in serum (Fig. 6a). These results revealed that granulocytes could be recruited and infiltrate the placenta after DENV-2 infection in pregnant mice.

Gene expression in placental cells was next analyzed by single-cell RNA sequencing, revealing 24 cell clusters. C5, C9, C11, and C20 had trophoblast characteristics (Fig. 6b). Based on reported cell markers,[55] clusters of trophoblast cells were identified and classified into three types: progenitor trophoblasts (C9), invasive spongiotrophoblasts (C5 and C11), and spiral artery trophoblast giant cells (C20). Compared with the uninfected group, the proportions of the above three types of trophoblast cells were notably decreased in the DENV-2-infected group, indicating a damaged structure of the placenta. C1, C3, C8 and C24 were identified as granulocytes, and their numbers were greatly increased after DENV-2 infection (Fig. 6b). *Itgam* and *Ly6g*, markers of neutrophils,[56] were expressed in all granulocyte subsets (Fig. 6c), whereas few cells among the four clusters expressed markers of eosinophils (*Ccr3*, *Il5ra*, and

perfusion of veins and arteries, respectively. Yellow dotted lines are used to outline the placentas. (e) Quantification of hemodynamics of umbilical artery. PSV, peak systolic velocity; EDV, end diastolic velocity; VTI, velocity time integral; MV, mean velocity; PI, pulsatility index; RI, resistance index. N = 6 per group. Data are presented as the mean ± SD (c and e). The significance of differences was analyzed by one-way ANOVA with a Tukey's multiple comparison test (c) or Bonferroni's multiple comparison test (e).

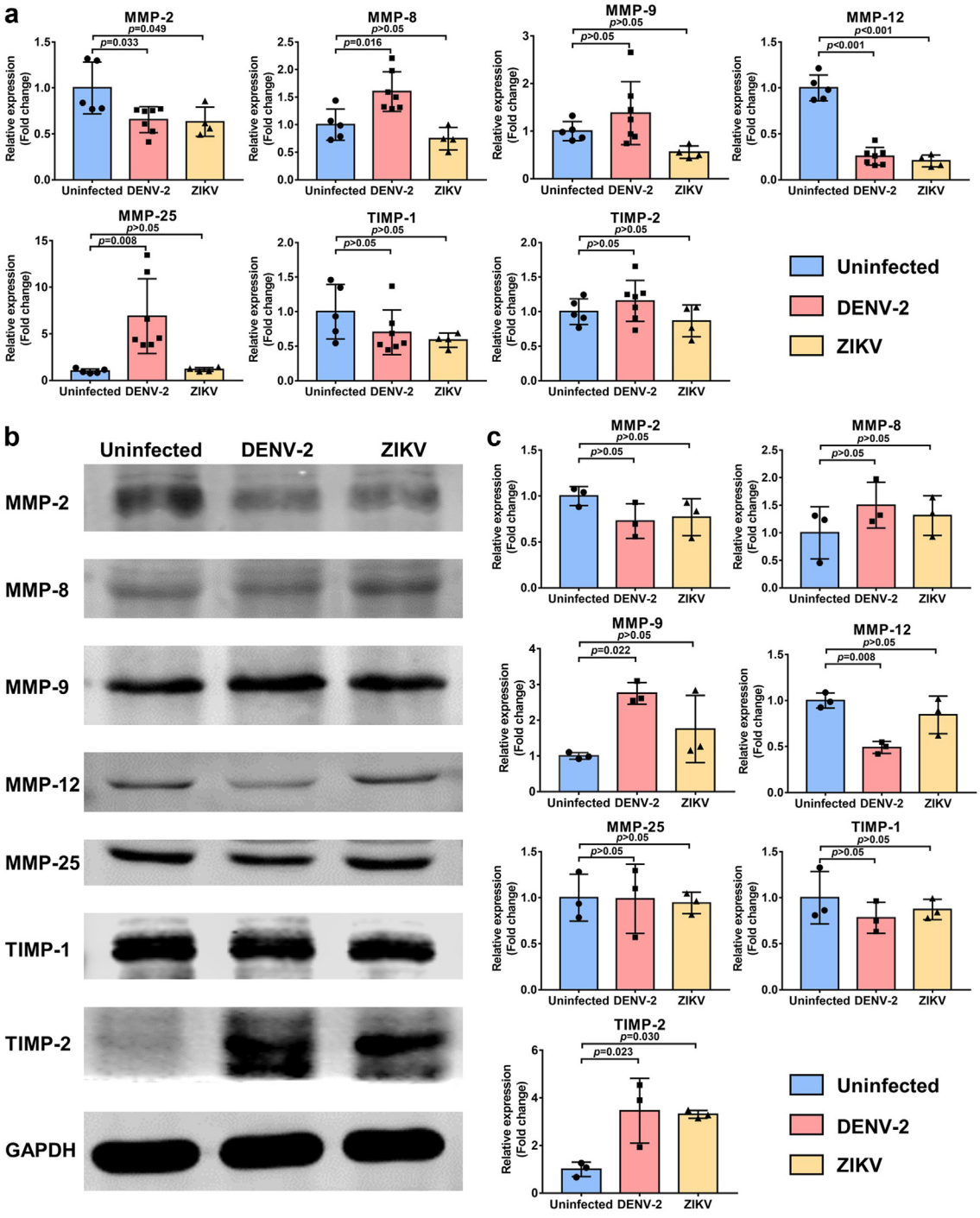


***Fig. 5:*** **The expression of extracellular matrix in gene and protein levels in the placentas.** Pregnant dams were subcutaneously inoculated with $10^5$ PFU DENV-2 or $10^4$ PFU ZIKV on E12.5. The placentas were collected at 6dpi. (a) The changes in the relative mRNA levels of key regulators of extracellular matrix were determined at 6 dpi by qRT-PCR. MMP, matrix metalloproteinase; TIMP, tissue inhibitor of metalloproteinase. N = 4 - 7 per group. (b) Representative image of Western blot analyzing MMPs in protein levels. (c) The relative expression levels of MMPs or TIMPs (target proteins/GAPDH) were further analyzed by measuring band density. N = 3 per group. Data are presented as the mean ± SD (a and c). The significance of differences was analyzed by ordinary one-way ANOVA with a Bonferroni's multiple comparison test (a) and a Tukey's multiple comparisons test (c).

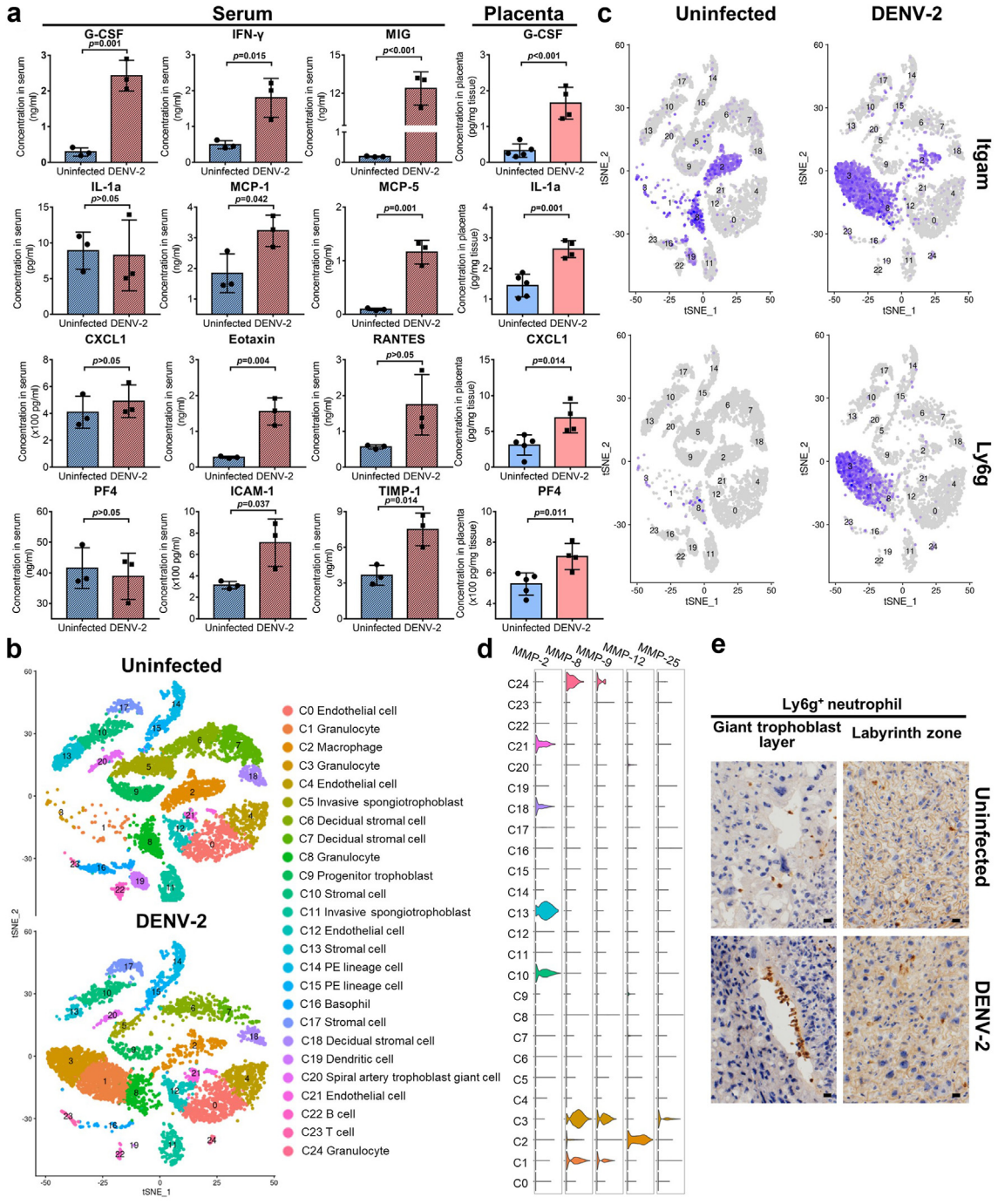


***Fig. 6:* A large number of neutrophils infiltrate into the placentas in DENV-2-infected *Ifnar1*$^{-/-}$ mice.** Pregnant dams were subcutaneously inoculated with $10^5$ PFU DENV-2 on E12.5. The serum and placentas were collected at 6dpi and subjected to cytokine analysis by quantitative inflammation array or single-cell RNA sequencing. There were three placentas from three individual pregnant mice in each group. Uninfected placentas were considered as control. (a) The levels of cytokines in serum or granulocyte chemokines in placentas. N = 3-5 per group. Data are presented as the mean ± SD. The significance of differences was analyzed by unpaired t test. (b) A t-SNE map of E18.5 mouse placenta single-cell data. Cells are colored by cell-type cluster. (c) t-SNE maps of placental single-cell data with cells colored based on the expression of marker genes for neutrophils. The expression levels of *Itgam* and *Ly6g* are indicated by shades of blue. (d) Violin plots details that the expression of MMP-8, MMP-9, and MMP-25 are mainly from granulocyte cluster. (e) Anti-Ly6g IHC staining reveals neutrophil infiltration into placentas after infection. Scale Bar = 20 μm.

*Siglecf*) and basophils (*Cd200r3*, *Fcer1a*, and *Mcpt8*) (Supplemental Figure S5). These results suggested that DENV-2 infection induced the infiltration of neutrophils into the placenta.

Furthermore, gene localization analysis revealed that MMP-8, MMP-9, and MMP-25 were mostly expressed in the granulocyte cluster; MMP-12 in the macrophage cluster; and MMP-2 in the stromal and endothelial cell clusters (Fig. 6d). Ly6g, exclusively expressed in murine neutrophils, was used to label neutrophils. IHC staining of the placentas with anti-Ly6g antibody revealed that, in contrast to uninfected mice, neutrophils were mainly aggregated in the giant cell trophoblast layer and were dispersed in the labyrinth zone after DENV-2 infection (Fig. 6e) or ZIKV infection (Supplemental Figure S6). These results indicated that the granulocyte chemokines induced by DENV-2 infection could cause abnormal infiltration of neutrophils, which further interfered with the expression of MMPs and placental vascularization.

### Sivelestat can alleviate fetal IUGR caused by DENV-2 infection in pregnant mice

Sivelestat is a competitive inhibitor of neutrophil elastase (NE) and has been approved for clinical use. To further determine whether neutrophils played an important role in the placental vascular damage induced by DENV-2 infection, pregnant dams were subcutaneously infected with $10^5$ PFU DENV-2 at E12.5, followed by an intraperitoneal injection of sivelestat. As a control, mice were injected with the same volume of PBS at the same time point. Compared with those of the PBS control group, the body weight loss in sivelestat-treated mice was alleviated, the average weight of the conceptus was increased, and the placental and fetal weights were modestly increased. However, treatment with sivelestat did not obviously improve the symptoms, and the ratio of placental weight to fetal weight remained high (Fig. 7a and b and Supplemental Figure S7a).

Histomorphological examination revealed that treatment with sivelestat restored placental perfusion in DENV-infected pregnant mice, particularly in the blood vessels in the giant cell trophoblast and labyrinth layers. The microvascular distribution in the labyrinth zone was relatively uniform (Fig. 7c). The vascular density and the number of branch points were increased (Fig. 7d and e). However, no overt differences in the viral loads of maternal major organs and the placenta were observed between the sivelestat-treated group and the PBS-control group, indicating that sivelestat may not dampen DENV replication (Supplemental Figure S7b). Taken together, these results suggested that sivelestat could alleviate vascular injury and improve placental perfusion, thereby mitigating but not eliminating the adverse effects caused by DENV-2 infection in pregnant mice.

### The placentas of DENV-infected pregnant women also showed damaged villi and abnormal vascular morphology

The placental tissues of three healthy pregnant women and two pregnant women infected with DENV in the third trimester were collected and evaluated for histomorphological changes. In the uninfected group, the placentas were well perfused and showed normal chorionic villi that included syncytiotrophoblasts, cytotrophoblasts and endothelial cells. In contrast, the placental villi in the DENV-infected women were severely damaged and presented with severe ischemic lesions, focal fibrin deposits and villous hypoplasia (Fig. 8). IHC staining of CD34 showed that the placental villi microvessels of uninfected pregnant women were uniform in size and distribution (Fig. 8). Compared with that of the uninfected group, the morphology of the placental villi varied greatly in DENV-infected patients; absent luminal spaces and irregular vascular walls were observed in a large number of blood vessels. Additionally, CD66b was used to localize granulocytes in the placentas. In uninfected cases, the granulocytes were scattered in the villus layer, but in contrast, they aggregated in the placentas of DENV-infected women (Fig. 8). These results suggested that DENV infection during the third trimester of pregnancy may also induce unusual aggregation of granulocytes, resulting in vascular damage to placental villi.

## Discussion

ZIKV infection is linked to severe pregnancy outcomes, and the discovery of the teratogenic consequences of ZIKV infection prompted us to refocus on the impact of other flavivirus infections on pregnancy. Unlike ZIKV causing fetal microcephaly by vertical transmission, preterm delivery, IUGR, or characteristic dengue fever symptoms in newborns are among the most prevalent unfavorable consequences of maternal DENV infection, which are definitely related to higher maternal and fetal morbidity and death.[2–4] In terms of pathogenesis, ZIKV has obvious neurotropism and can directly infect neurons in the fetal brain. However, adverse pregnancy outcomes caused by maternal DENV infection are more relevant to the pathophysiological changes in the placenta. DENV infection has progressed to the pandemic stage, with pregnant women being at high risk. The mechanism by which DENV infection leads to adverse pregnancy outcomes needs to be further illustrated.

In this study, we demonstrate that DENV-2 infection in pregnant *Ifnar1*$^{-/-}$ mice causes severe fetal growth restriction, manifested by lower body weight, anemia, and multiple organ retardation. Placental histomorphological examination suggested trophoblast giant cell necrosis in the junctional zone and loss of microvessels in the labyrinth zone, which may lead to inadequate

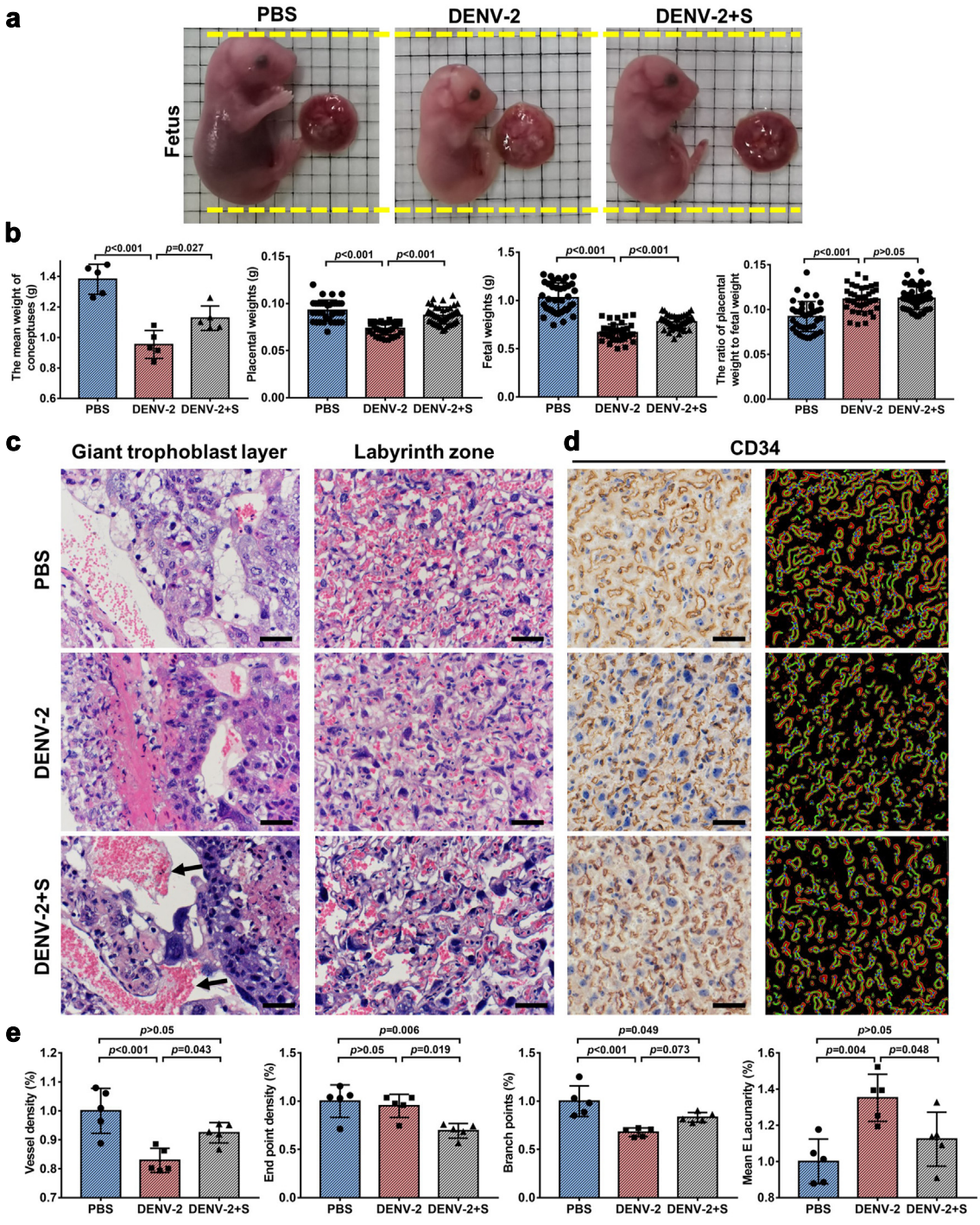


*Fig. 7:* **Sivelestat alleviates fetal growth restriction caused by DENV-2 infection.** Pregnant dams were subcutaneously inoculated with $10^5$ PFU DENV-2 on E12.5, followed by treatment with intraperitoneal injection of sivelestat (100 mg/kg). Mice injected with the same volume of PBS were used as untreated control. Mice were sacrificed at 6 dpi and the conceptuses were collected. (a) Representative images of fetuses and placentas of E18.5 dams. (b) The changes of mean weights of conceptuses, placental weights, fetal weights, and the ratio of placental weight to fetal weight in pregnant mice injected with PBS, DENV-2, or DENV-2 plus sivelestat (DENV-2+S) were evaluated. Each spot represents an individual pregnant mouse (the left panel) or an individual fetus (the three panels on the right). Fetuses in each group were carried by 5 pregnant dams. N = 38 - 46 in each group. (c) Histopathological changes were analyzed by HE staining. Arrow indicates fully perfused blood vessels. Scale bar = 100 μm. (d) CD34 expression in placental labyrinth zone was assessed by IHC staining after injection of PBS, DENV-2, or

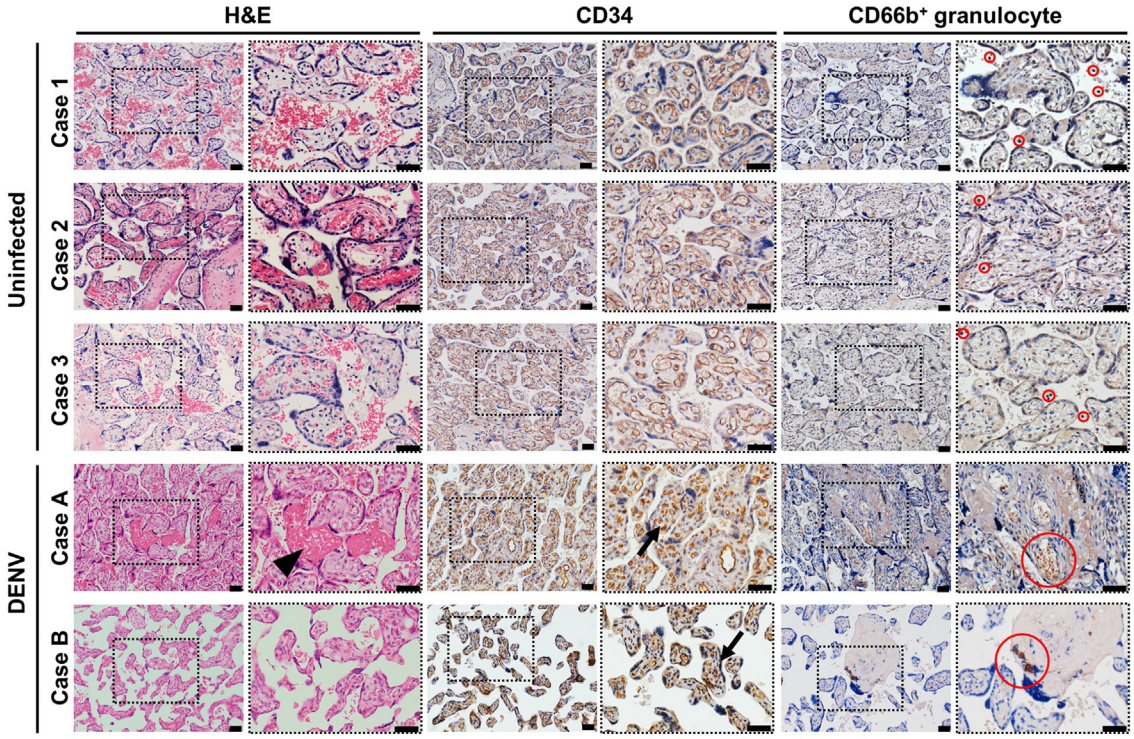


*Fig. 8:* **Histopathological changes of placentas of DENV-infected pregnant women.** Representative images of placentas stained by HE. Arrowhead indicates necrosis (the left panel). CD34 expression in placental villi was examined by IHC staining. Arrow indicates closed vessel (the middle panel). Anti-CD66b IHC staining reveals abnormal neutrophil aggregation in the placentas of DENV-infected women (the right panel); scattered neutrophils (small cycles), aggregated neutrophils (big cycles). Scale bar = 50 μm.

oxygenation or delivery of nutrients to the fetal tissues, thereby contributing to potential developmental restriction of fetuses. Changes in placental histomorphology were also found in the ZIKV-infected group, which was consistent with previous studies.[57] However, fetal viral infection can only be detected in ZIKV-infected dams rather than DENV-2-infected dams. These findings indicate that after DENV-2 infection, placental pathophysiological changes causing placental insufficiency rather than viral transmission probably play a leading role in the profound deleterious fetal outcome in this model. However, in the case of ZIKV infection, fetal IUGR may be mainly attributed to direct damage of the virus to the fetus followed by pathophysiological changes in placental function.

In fact, vertical transmission of dengue is not thought to be common, although the virus and antibodies against the virus have been found in placentas, in the cord blood of infants, and in the lung and kidney cells of an aborted fetus.[17,58–62] Vertical transmission includes transplacental transmission and transvaginal transmission, which differ greatly with respect to their pathophysiological processes. It has been solidly shown that ZIKV can spread transplacentally,[63] whereas DENV does not in our model. Further research is required to clarify the mechanism underlying DENV infection in neonates born from women infected with DENV in the last trimester or close to term.[19]

To verify the above histopathological changes in the placenta, the impact of maternal DENV infection on placental tissue was further investigated in patients. Both cases showed highly similar histopathological changes, including hypoperfusion, focal fibrin deposits, damaged vasculature, and leukocyte infiltration, which were consistent with the observations in a previous study[7] and in our mouse model. These changes could contribute to abnormal placental hemodynamics during pregnancy, causing fetal nutritional deficiency and hypoxia.

DENV-2 plus sivelestat (DENV-2+S). CD34-positive microvessels were visualized by AngioTool software. Scale bar = 100 μm. (e) Quantification of vessel density, end point density, branch points, and mean lacunarity in placental labyrinth zone. N = 5 per group. Data are presented as the mean ± SD (b and e). The significance of differences was analyzed by ordinary one-way ANOVA with a Bonferroni's multiple comparison test (b, right three panel) and a Tukey's multiple comparisons test (b, left one panel; e).

In reproductive biology, neutrophils are rapidly emerging as key players, and their functions include promoting implantation, spiral artery modification and even assisting with the process of parturition.[13] However, uncontrolled neutrophil activation is a hallmark of inflammation, resulting in tissue damage and dysfunction, which may be related to severe pregnancy complications ranging from preeclampsia to fetal loss.[64] In this study, we found that vascular endothelial cells and leukocytes in the placenta were infected by DENV-2 and that granulocyte chemokines were significantly increased in the placenta. These results suggest a mechanism by which infected endothelial cells and leukocytes release massive neutrophil chemoattractants, thereby breaking up inherent placental immune homeostasis. Furthermore, the interactions between neutrophils and endothelial cells induce inflammatory cytokine and chemokine production by placental endothelial cells, which furthers neutrophil recruitment and activation, thus establishing a self-amplifying loop of inflammation.[14,65] Such neutrophil infiltration was also observed in other pregnancy infections, including cytomegalovirus, *Listeria*, and *U. parvum*.[66–68] However, our study provided important clues for clarifying the specific mechanism of DENV-associated fetal growth restriction.

Neutrophils contain a large variety of proteases, and excessive accumulation in the placenta plays a deleterious role in interfering with placental vascularization, trophoblast invasion and differentiation and even affects trophoblast survival by upregulating the expression of specific proteases and anomalous profiles of MMPs.[13,15] In this study, the upregulation of MMP-8, -9, and -25, mainly derived from neutrophils, may degrade the basal lamina of vessels in the placenta, which suggests that DENV infection destroys the remodeling of the ECM, potentially affecting the integrity of the placenta. Moreover, the permeability of endothelial cells during DENV infection could be impaired, and such failure results in inadequate oxygenation or delivery of nutrients from the placenta to fetal tissues, thereby contributing to the pathogenesis of IUGR. Although neutrophils were the most frequent immunocytes in the placenta in response to DENV infection in this study, other immunocytes may also play an active role in destroying the placental structure, which needs more attention.

Sivelestat, a selective neutrophil elastase inhibitor, was used for the clinical treatment of acute lung injury and acute respiratory distress syndrome.[69] In fact, sivelestat not only inhibits the activity of elastase but also mitigates neutrophil-mediated organ damage.[70] In this study, to inhibit the function of neutrophils in the placenta, DENV-2-infected pregnant mice were treated with sivelestat. Although the administration of sivelestat did not influence viral replication, it effectively alleviated placental microvascular damage and fetal growth restriction, further suggesting that after DENV-2 infection, fetal IUGR is caused by placental neutrophil infiltration and its destructive effects on the placental vasculature. Sivelestat has few adverse effects on fetal development and maternal health in rats[71] and humans, and it is licensed for clinical use for the treatment of acute lung injury associated with systemic inflammatory response syndrome in Japan.[72] This approach may provide a new perspective for treating severe complications caused by DENV infection in pregnant women.

A previous study showed that DENV-3 infection did not result in placental damage or fetal pathology, and another indicated that DENV can be transmitted vertically in a gestation stage-dependent manner similar to ZIKV.[43,73,74] The difference in the results between our study and the literature was likely related to different mouse models, inoculation routes, pregnancy stages, virulence among serotypes, and viral doses used, which are all important influencing factors of adverse pregnancy outcomes during DENV infection in pregnant mice. Our findings demonstrate the potential for DENV infection to cause critical fetal outcomes during pregnancy and elucidate the possible pathogenesis. However, there are some limitations. First, our results were obtained by using immunocompromised mice, and the absence of type I IFN signaling may affect placental barrier defenses and integrity.[75,76] Consequently, the use of this model may amplify the effect of DENV infection on fetal development and placental histopathology. Therefore, caution is needed when using mouse results to represent human diseases. Second, although it is widely accepted that the mouse can serve as a useful model for pregnancy-related diseases in humans, the placental histomorphology and exchange physiology in humans and mice are different. For example, distinct cellular components of the fetal–maternal interface in the placenta may make it challenging to directly extrapolate the results from mouse placental studies to humans.[10] Although similar changes in the placental vasculature were observed in placental tissues from women undergoing pregnancy termination after DENV infection, other examinations, such as changes in cytokines and MMPs, were not carried out due to the limited numbers of human placental tissue samples. Different from mouse samples, it was difficult to harvest sufficient placental tissues from pregnant women infected with DENV in the third trimester. Therefore, in this study, primary experiments were conducted in the mouse model, followed by further confirmation in human samples. Unusual granulocyte aggregation and damaged placental vasculature in human placental sections add to our concerns about DENV causing severe pregnancy outcomes. We hope that the findings of this study will attract more clinician's attention and more human placenta samples will be collected to further investigate this scientific subject in the population. Moreover, it should be noted that whether the underlying mechanism of other adverse pregnancy outcomes caused by DENV infection, including stillbirth,

miscarriage, and preterm birth, is similar to that of fetal growth restriction also needs further investigation.

In conclusion, our study revealed that placental immunopathological lesions and insufficiency can contribute to DENV-associated adverse fetal outcomes independent of direct viral damage within developing embryos in *Ifnar1*$^{-/-}$ pregnant mice. The unusual aggregation of granulocytes in the placenta resulted in abnormal expression of MMPs that could affect placental vascularization, which may interfere with feto-maternal exchange and ultimately lead to fetal intrauterine growth restriction (Supplemental Figure S8). Sivelestat, an agent inhibiting the function of neutrophils, may provide new insight into the therapy of DENV-associated adverse pregnancy outcomes.

#### Contributors

J. A., F. L. and Z. S. designed the experiments. Y. Z. and Z. S. performed the majority of the experiments. J. C., F. X. and Y. L. assisted in collection of experimental materials. A. Z. helped to analyze the histopathological examinations. F. L., Q. C., Y. Y., L. Liang. and F. Z. provided human samples. N. W., N. G. and D. F. provided key reagents or experimental advice. P. W., D. Z. and L. Liu. helped to analyze the data. Y. Z. wrote the manuscript and J. A. and Z. S. revised the manuscript with other authors providing editorial comments.

#### Data sharing statement

The data that support these findings of the study are available upon request from the corresponding authors.

#### Declaration of interests

We declare that we do not have any commercial or associative interest that represents a conflict of interest in connection with the work submitted.

#### Acknowledgements

This work was funded by the grants from the National Key Research and Development Program of China (2021YFC2300200-02 to J.A., 2019YFC0121905 to Q.Z.C.), the National Natural Science Foundation of China (NSFC) (U1902210 and 81972979 to J. A., 81902048 to Z. Y. S., and 82172266 to P.G.W.), and the Support Project of High-level Teachers in Beijing Municipal Universities in the Period of 13th Five-year Plan, China (IDHT20190510 to J. A.).

#### Appendix A. Supplementary data

Supplementary data related to this article can be found at https://doi.org/10.1016/j.ebiom.2023.104739.

#### References

1 Pierson TC, Diamond MS. The continued threat of emerging flaviviruses. *Nat Microbiol*. 2020;5(6):796–812.
2 Ribeiro IM, Souto PCS, Borbely AU, et al. The limited knowledge of placental damage due to neglected infections: ongoing problems in Latin America. *Syst Biol Reprod Med*. 2020;66(3):151–169.
3 Paixao ES, Harron K, Campbell O, et al. Dengue in pregnancy and maternal mortality: a cohort analysis using routine data. *Sci Rep*. 2018;8(1):9938.
4 Kallur SD, Surapaneni T, Boorugu HK, Aziz N, Gala AR, Donnuri S. Need for guidelines for the combined management of pregnancy and dengue: a retrospective study from an Indian tertiary care maternity hospital. *Trop Doct*. 2019;49(1):7–9.
5 Paixao ES, Teixeira MG, Costa M, Rodrigues LC. Dengue during pregnancy and adverse fetal outcomes: a systematic review and meta-analysis. *Lancet Infect Dis*. 2016;16(7):857–865.
6 Pouliot SH, Xiong X, Harville E, et al. Maternal dengue and pregnancy outcomes: a systematic review. *Obstet Gynecol Surv*. 2010;65(2):107–118.
7 Ribeiro CF, Lopes VGS, Brasil P, Pires ARC, Rohloff R, Nogueira RMR. Dengue infection in pregnancy and its impact on the placenta. *Int J Infect Dis*. 2017;55:109–112.
8 Yang J, Zhang J, Deng Q, et al. Investigation on prenatal dengue infections in a dengue outbreak in Guangzhou City, China. *Infect Dis (Lond)*. 2017;49(4):315–317.
9 Kourtis AP, Read JS, Jamieson DJ. Pregnancy and infection. *N Engl J Med*. 2014;370(23):2211–2218.
10 Rossant J, Cross JC. Placental development: lessons from mouse mutants. *Nat Rev Genet*. 2001;2(7):538–548.
11 Cox B, Kotlyar M, Evangelou AI, et al. Comparative systems biology of human and mouse as a tool to guide the modeling of human placental pathology. *Mol Syst Biol*. 2009;5:279.
12 Dilworth MR, Sibley CP. Review: transport across the placenta of mice and women. *Placenta*. 2013;34(Suppl):S34–S39.
13 Giaglis S, Stoikou M, Grimolizzi F, et al. Neutrophil migration into the placenta: good, bad or deadly? *Cell Adh Migr*. 2016;10(1-2):208–225.
14 Mayadas TN, Cullere X, Lowell CA. The multifaceted functions of neutrophils. *Annu Rev Pathol*. 2014;9:181–218.
15 Bert S, Ward EJ, Nadkarni S. Neutrophils in pregnancy: new insights into innate and adaptive immune regulation. *Immunology*. 2021;164(4):665–676.
16 Nunes P, Nogueira R, Coelho J, et al. A stillborn multiple organs' investigation from a maternal DENV-4 infection: histopathological and inflammatory mediators characterization. *Viruses*. 2019;11(4).
17 Ribeiro CF, Lopes VG, Brasil P, Coelho J, Muniz AG, Nogueira RM. Perinatal transmission of dengue: a report of 7 cases. *J Pediatr*. 2013;163(5):1514–1516.
18 Charlier C, Beaudoin MC, Couderc T, Lortholary O, Lecuit M. Arboviruses and pregnancy: maternal, fetal, and neonatal effects. *Lancet Child Adolesc Health*. 2017;1(2):134–146.
19 Basurko C, Matheus S, Hilderal H, et al. Estimating the risk of vertical transmission of dengue: a prospective study. *Am J Trop Med Hyg*. 2018;98(6):1826–1832.
20 Marin-Lopez A, Calvo-Pinilla E, Moreno S, et al. Modeling arboviral infection in mice lacking the interferon alpha/beta receptor. *Viruses*. 2019;11(1):35.
21 Sarathy VV, Milligan GN, Bourne N, Barrett AD. Mouse models of dengue virus infection for vaccine testing. *Vaccine*. 2015;33(50):7051–7060.
22 Coyne CB, Lazear HM. Zika virus - reigniting the TORCH. *Nat Rev Microbiol*. 2016;14(11):707–715.
23 Charan J, Kantharia ND. How to calculate sample size in animal studies? *J Pharmacol Pharmacother*. 2013;4(4):303–306.
24 An J, Kimura-Kuroda J, Hirabayashi Y, Yasui K. Development of a novel mouse model for dengue virus infection. *Virology*. 1999;263(1):70–77.
25 An J, Zhou DS, Kawasaki K, Yasui K. The pathogenesis of spinal cord involvement in dengue virus infection. *Virchows Arch*. 2003;442(5):472–481.
26 Ma W, Li S, Ma S, et al. Zika virus causes Testis damage and leads to male infertility in mice. *Cell*. 2016;167(6):1511–1524.e10.
27 Wang Q, Yang Y, Zheng H, et al. Genetic and biological characterization of Zika virus from human cases imported through Shenzhen Port. *Chin Sci Bull*. 2016;61(0023-074X):2463.
28 Zudaire E, Gambardella L, Kurcz C, Vermeren S. A computational tool for quantitative analysis of vascular networks. *PLoS One*. 2011;6(11):e27385.
29 Sheng ZY, Gao N, Wang ZY, et al. Sertoli cells are susceptible to ZIKV infection in mouse Testis. *Front Cell Infect Microbiol*. 2017;7:272.
30 Wu W, Peng S, Shi Y, Li L, Song Z, Lin S. NPY promotes macrophage migration by upregulating matrix metalloproteinase-8 expression. *J Cell Physiol*. 2021;236(3):1903–1912.
31 Shiryaev SA, Remacle AG, Savinov AY, et al. Inflammatory proprotein convertase-matrix metalloproteinase proteolytic pathway in antigen-presenting cells as a step to autoimmune multiple sclerosis. *J Biol Chem*. 2009;284(44):30615–30626.
32 Mota R, Parry TL, Yates CC, et al. Increasing cardiomyocyte atrogin-1 reduces aging-associated fibrosis and regulates remodeling in vivo. *Am J Pathol*. 2018;188(7):1676–1692.
33 Sosne G, Christopherson PL, Barrett RP, Fridman R. Thymosin-beta 4 modulates corneal matrix metalloproteinase levels and polymorphonuclear cell infiltration after alkali injury. *Invest Ophthalmol Vis Sci*. 2005;46(7):2388–2395.
34 Zhang H, Mao YF, Zhao Y, et al. Upregulation of matrix metalloproteinase-9 protects against sepsis-induced acute lung

injury via promoting the release of soluble receptor for advanced glycation end products. *Oxid Med Cell Longev*. 2021;2021:8889313.
35 Stronati L, Palone F, Negroni A, et al. Dipotassium glycyrrhizate improves intestinal mucosal healing by modulating extracellular matrix remodeling genes and restoring epithelial barrier functions. *Front Immunol*. 2019;10:939.
36 Hayward CE, Lean S, Sibley CP, et al. Placental adaptation: what can we learn from birthweight:placental weight ratio? *Front Physiol*. 2016;7:28.
37 Mitsuda N, J-P NA, Eitoku M, et al. Association between maternal hemoglobin concentration and placental weight to birthweight ratio: the Japan Environment and Children's Study (JECS). *Placenta*. 2020;101:132–138.
38 Besnard AE, Wirjosoekarto SA, Broeze KA, Opmeer BC, Mol BW. Lecithin/sphingomyelin ratio and lamellar body count for fetal lung maturity: a meta-analysis. *Eur J Obstet Gynecol Reprod Biol*. 2013;169(2):177–183.
39 Kastl JT. Renal function in the fetus and neonate - the creatinine enigma. *Semin Fetal Neonatal Med*. 2017;22(2):83–89.
40 Terada T, Nakanuma Y. Expression of pancreatic enzymes (alpha-amylase, trypsinogen, and lipase) during human liver development and maturation. *Gastroenterology*. 1995;108(4):1236–1245.
41 Megli CJ, Coyne CB. Infections at the maternal-fetal interface: an overview of pathogenesis and defence. *Nat Rev Microbiol*. 2022;20(2):67–82.
42 Vermillion MS, Lei J, Shabi Y, et al. Intrauterine Zika virus infection of pregnant immunocompetent mice models transplacental transmission and adverse perinatal outcomes. *Nat Commun*. 2017;8:14575.
43 Miner JJ, Cao B, Govero J, et al. Zika virus infection during pregnancy in mice causes placental damage and fetal demise. *Cell*. 2016;165(5):1081–1091.
44 Wang L, Sun L, Gu Z, et al. N-carboxymethyl chitosan/sodium alginate composite hydrogel loading plasmid DNA as a promising gene activated matrix for in-situ burn wound treatment. *Bioact Mater*. 2022;15:330–342.
45 Chen J, Khalil RA. Matrix metalloproteinases in normal pregnancy and preeclampsia. *Prog Mol Biol Transl Sci*. 2017;148:87–165.
46 Li J, Quan X, Zhang Y, et al. PPARgamma regulates triclosan induced placental dysfunction. *Cells*. 2021;11(1):86.
47 Dias-Junior CA, Chen J, Cui N, et al. Angiogenic imbalance and diminished matrix metalloproteinase-2 and -9 underlie regional decreases in uteroplacental vascularization and feto-placental growth in hypertensive pregnancy. *Biochem Pharmacol*. 2017;146:101–116.
48 Radisky ES, Raeeszadeh-Sarmazdeh M, Radisky DC. Therapeutic potential of matrix metalloproteinase inhibition in breast cancer. *J Cell Biochem*. 2017;118(11):3531–3548.
49 Eckfeld C, Haussler D, Schoeps B, Hermann CD, Kruger A. Functional disparities within the TIMP family in cancer: hints from molecular divergence. *Cancer Metastasis Rev*. 2019;38(3):469–481.
50 Roberts AW. G-CSF: a key regulator of neutrophil production, but that's not all. *Growth Factors*. 2005;23(1):33–41.
51 Engstad CS, Lia K, Rekdal O, Olsen JO, Osterud B. A novel biological effect of platelet factor 4 (PF4): enhancement of LPS-induced tissue factor activity in monocytes. *J Leukoc Biol*. 1995;58(5):575–581.
52 Lee PY, Kumagai Y, Xu Y, et al. IL-1 alpha modulates neutrophil recruitment in chronic inflammation induced by hydrocarbon oil. *J Immunol*. 2011;186(3):1747–1754.
53 Sawant KV, Poluri KM, Dutta AK, et al. Chemokine CXCL1 mediated neutrophil recruitment: role of glycosaminoglycan interactions. *Sci Rep*. 2016;6:33123.
54 Borregaard N. Neutrophils, from marrow to microbes. *Immunity*. 2010;33(5):657–670.
55 Han X, Wang R, Zhou Y, et al. Mapping the mouse cell atlas by microwell-seq. *Cell*. 2018;172(5):1091–1107.e17.
56 Nguyen CT, Furuya H, Das D, et al. Peripheral gammadelta T cells regulate neutrophil expansion and recruitment in experimental psoriatic arthritis. *Arthritis Rheumatol*. 2022;74:1524.
57 Szaba FM, Tighe M, Kummer LW, et al. Zika virus infection in immunocompetent pregnant mice causes fetal damage and placental pathology in the absence of fetal infection. *PLoS Pathog*. 2018;14(4):e1006994.
58 Ventura AK, Ehrenkranz NJ, Rosenthal D. Placental passage of antibodies to Dengue virus in persons living in a region of hyperendemic Dengue virus infection. *J Infect Dis*. 1975;131(Suppl):S62–S68.
59 Paixao ES, Costa M, Teixeira MG, et al. Symptomatic dengue infection during pregnancy and the risk of stillbirth in Brazil, 2006-12: a matched case-control study. *Lancet Infect Dis*. 2017;17(9):957–964.
60 Perret C, Chanthavanich P, Pengsaa K, et al. Dengue infection during pregnancy and transplacental antibody transfer in Thai mothers. *J Infect*. 2005;51(4):287–293.
61 Argolo AF, Feres VC, Silveira LA, et al. Prevalence and incidence of dengue virus and antibody placental transfer during late pregnancy in central Brazil. *BMC Infect Dis*. 2013;13:254.
62 Leite RC, Souza AI, Castanha PM, et al. Dengue infection in pregnancy and transplacental transfer of anti-dengue antibodies in Northeast, Brazil. *J Clin Virol*. 2014;60(1):16–21.
63 Mlakar J, Korva M, Tul N, et al. Zika virus associated with microcephaly. *N Engl J Med*. 2016;374(10):951–958.
64 Hahn S, Giaglis S, Hoesli I, Hasler P. Neutrophil NETs in reproduction: from infertility to preeclampsia and the possibility of fetal loss. *Front Immunol*. 2012;3:362.
65 DiStasi MR, Ley K. Opening the flood-gates: how neutrophil-endothelial interactions regulate permeability. *Trends Immunol*. 2009;30(11):547–556.
66 McDonagh S, Maidji E, Chang HT, Pereira L. Patterns of human cytomegalovirus infection in term placentas: a preliminary analysis. *J Clin Virol*. 2006;35(2):210–215.
67 Xu L, Du Y, Wu Y. Neglected listeria infection in pregnancy in China: 93 cases. *J Matern Fetal Neonatal Med*. 2022:1–9.
68 von Chamier M, Allam A, Brown MB, Reinhard MK, Reyes L. Host genetic background impacts disease outcome during intrauterine infection with Ureaplasma parvum. *PLoS One*. 2012;7(8):e44047.
69 Kido T, Muramatsu K, Yatera K, et al. Efficacy of early sivelestat administration on acute lung injury and acute respiratory distress syndrome. *Respirology*. 2017;22(4):708–713.
70 Al-Kuraishy HM, Al-Gareeb AI, Al-Hussaniy HA, Al-Harcan NAH, Alexiou A, Batiha GE. Neutrophil Extracellular Traps (NETs) and Covid-19: a new frontiers for therapeutic modality. *Int Immunopharmacol*. 2022;104:108516.
71 Nishimura T, Chihara N, Shirakawa R, et al. [Reproductive and developmental toxicity studies of landiolol hydrochloride (ONO-1101) (4). Perinatal and postnatal study in rats]. *J Toxicol Sci*. 1997;22(Suppl 3):537–557.
72 Nakajima Y, Masaoka N. Initial experience using Sivelestat to manage preterm labor with a bulging fetal membrane in pregnant women. *J Perinatol*. 2012;32(6):466–468.
73 Jaeger AS, Weiler AM, Moriarty RV, et al. Spondweni virus causes fetal harm in Ifnar1(-/-) mice and is transmitted by Aedes aegypti mosquitoes. *Virology*. 2020;547:35–46.
74 Watanabe S, Chan KWK, Tan NWW, et al. Experimental evidence for a high rate of maternal-fetal transmission of dengue virus in the presence of antibodies in immunocompromised mice. *eBioMedicine*. 2022;77:103930.
75 Kwon JY, Aldo P, You Y, et al. Relevance of placental type I interferon beta regulation for pregnancy success. *Cell Mol Immunol*. 2018;15(12):1010–1026.
76 Wells AI, Coyne CB. Type III interferons in antiviral defenses at barrier surfaces. *Trends Immunol*. 2018;39(10):848–858.